

电子束钎焊温度模糊控制系统

王学东， 姚 舜

(上海交通大学 材料科学与工程学院 上海 200030)



王学东

摘 要：将被焊工件温度模糊控制技术应用于电子束扫描钎焊中，所研发的系统集成电子束焊接过程控制、电子束扫描轨迹控制、工件温度模糊控制、焊接数据高速采集与存储等多项功能。通过扫描轨迹的编辑与控制，可以适应各种形状曲线钎焊缝的温度场要求；在电子束对工件进行扫描加热的同时，通过温度采集装置实时得到被焊工件的温度信号并与设定值进行对比从而得到温度偏差及偏差的变化率作为模糊控制器的两个输入变量，以模糊控制器输出控制量调节电子束流大小，从而实现钎焊温度的闭环控制。控制系统具有响应速度快、稳定时间短、稳态误差小、超调量小等特点，表明在电子束钎焊过程中采用模糊控制技术可以得到非常理想的控制效果。

关键词：电子束钎焊；扫描轨迹；温度闭环控制；模糊控制

中图分类号：TG156 文献标识码：A 文章编号：0253-360X(2006)05-073-04

0 序 言

真空电子束焊接以其高能量密度、深穿透、真空焊接、精密控制、高速扫描、高速加热等优势，使其在特殊材料、新结构制造的应用中具有广阔的前景^[1~3]。在空间推进系统发动机的各种精密、复杂部件加工中采用电子束钎焊，可大幅度提高钎焊结构的综合性能。

为了将电子束成功地应用于钎焊，首先它要能适应各种形状的曲线钎焊缝的加热要求，利用电子束扫描轨迹编辑和控制功能可满足这一要求^[4]。另一方面，由于钎焊温度是重要的钎焊工艺参数，特别是对热敏感性材料的电子束钎焊更是如此，但是由于电子束焊接在真空室中进行，能量密度高，工件温度变化快，控制难度大，因此需采用适合于电子束钎焊这种特点的温度场闭环控制方法。

模糊控制无需知道被控对象的数学模型，它是人对被控系统的控制经验为依据而设计的控制器。从焊接实践来看，电子束钎焊过程控制是有规律可循的，而且模糊控制具有良好的鲁棒性和适应性，因此在电子束钎焊过程中采用模糊控制技术必定具有广阔的前景。

目前，在电子束钎焊过程中采用任何形式的温

度闭环控制技术，国内外还未见有报道，而采用模糊控制技术则是崭新的尝试。

1 系统的组成

系统由电子束焊机、工业控制计算机、可编程序控制器、功率放大器、红外测温仪、偏转线圈、数据采集装置、AD/DA 转换器及控制软件等几部分构成。

焊前根据钎焊缝的形状及加工要求编辑电子束扫描轨迹及扫描方式，由工业控制计算机计算扫描轨迹所需波形数据，再由 D/A 转换器将其转变为模拟量，输出至功率放大器放大后，输入偏转线圈，在偏转线圈中产生的磁场使电子束按设定的扫描轨迹对工件进行加热；在电子束对工件扫描加热的同时，通过红外测温仪实时检测钎焊加热区温度。红外测温仪输出的信号通过数据采集装置采集后再经 A/D 转换，输入计算机，经模糊控制器处理并输出控制量，根据此控制量调节电子束流的大小，实现钎焊温度的精确控制。

2 扫描轨迹控制原理

电子束扫描轨迹采用 x 、 y 位移分量来描述，电子束从扫描轨迹的起始点运动到终点构成一个扫描周期，利用一个扫描周期的 x 、 y 位移分量，通过控

收稿日期：2005-02-01
基金项目：上海市科学技术委员会科研计划项目(036105001)；
国际科技合作重点项目(2004DFA02400)

制软件及 D/A 转换器生成两路模拟信号, 以指定的刷新率不断地输出给由 x 、 y 两对绕组构成的附加偏转线圈, 在附加偏转线圈中产生的磁场使电子束周期性地 在 $x-y$ 平面内按设定的轨迹和方式运动。图 1 所示为电子束扫描轨迹在计算机屏幕上的显示及在工件上扫描加热的实拍照片示例。

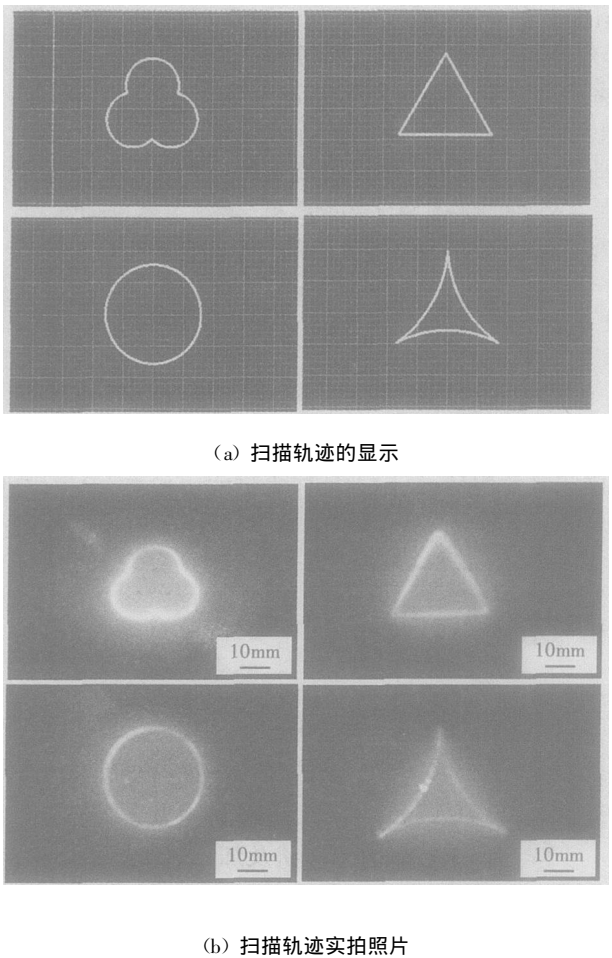


图 1 电子束扫描轨迹编辑及实拍照片示例
Fig. 1 Scanning tracks' display (upper row) and photographs(lower row)

3 模糊控制器的设计

模糊控制是以模糊集合论、模糊语言变量及模糊逻辑推理为基础的智能控制方法, 模糊控制系统的基本原理框图如图 2 所示。模糊控制器是它的核心部分, 其控制规律由计算机程序实现。

3.1 定义输入输出变量

钎焊系统控制的是被焊工件温度, 因此被焊工件温度设定值与被焊工件实际温度检测值的偏差量 e 为模糊控制器的一个输入量, 如图 2 所示。考虑到电子束钎焊能量密度高、工件温度对束流值很敏

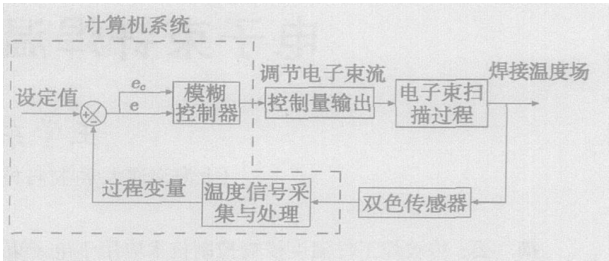


图 2 电子束钎焊模糊控制系统原理框图
Fig. 2 Schematic diagram of electron beam brazing fuzzy control system

感的特点, 因此模糊控制器另一个输入量为偏差的变化率 e_c ; 模糊控制器的输出 u 用于调节电子束流大小。因此, 系统采用的是单变量二维模糊控制器。
3.2 变量论域、量化等级、量化因子及隶属度函数的确定

变量论域要根据受控系统的实际情况来决定, 输入输出变量的论域分别取决于输入变量的测量范围和实际的控制作用范围, 主要是确定 e_c 和 u 的范围。对于这两个数据, 由于并无电子束钎焊模糊控制试验数据可供参考, 因此以作者前期所做的 PID 控制试验数据为参照并结合电子束钎焊模糊控制试验, 确定偏差 e 的论域为 $[-20, 20]$, 偏差变化率 e_c 的论域为 $[-100, 100]$, 控制器输出 u 的论域为 $[-40, 40]$ 。取 3 个语言变量的量化等级都为 7 级, 即 $\{-3, -2, -1, 0, 1, 2, 3\}$, e 、 e_c 及 u 的量化因子分别为 k_1 、 k_2 及 k_3 , 则 $k_1 = 3/20$, $k_2 = 3/100$, $k_3 = 40/3$ 。

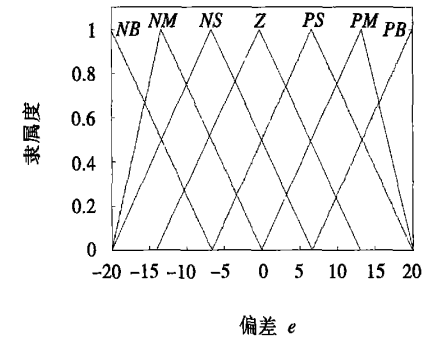
模糊控制器的隶属度函数通常有三角形、梯形、钟形等, 而大量经验表明, 采用三角形和梯形的隶属度函数会在实际应用中带来很多方便, 因此系统采用三角形隶属度函数。

大多数应用中, 根据具体要求的不同, 语言变量的取值范围为 3~7, 少于 3 个是不可取的, 而划分得过细反而会使控制规则变得过于复杂。为了得到较好的控制效果, 系统在各语言变量论域内, 都取 7 个模糊子集, 即 $NB, NM, NS, Z, PS, PM, PB$ 。各语言变量的隶属度函数如图 3 所示。

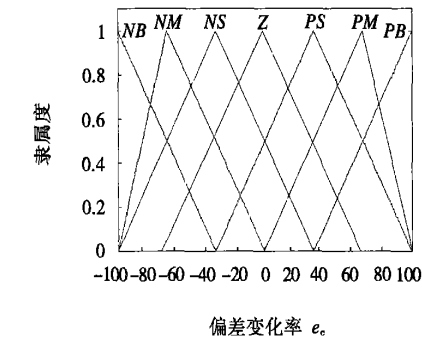
3.3 模糊控制规则的确定

模糊控制规则实质上是根据焊接操作人员的经验知识, 根据被焊工件温度的偏差及偏差的变化趋势来消除系统误差, 所以确定模糊控制规则的原则是必须保证控制器的输出能够使系统输出响应的动、静态特性达到最佳。

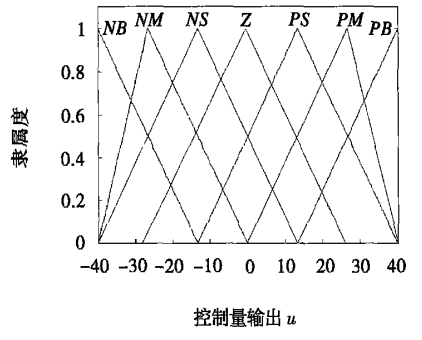
模糊控制规则可采用模糊规则表来描述, 如表 1 所示, 共 49 条模糊规则。



(a) e 的隶属函数图



(b) e_c 的隶属函数图



(c) u 的隶属函数图

图 3 输入与输出变量的隶属函数图

Fig. 3 Membership functions of input and output variables

表 1 模糊控制规则表

Table 1 Fuzzy control rules table

| e e_c | NB | NM | NS | ZO | PS | PM | PB |
|--------------|----|----|----|----|----|----|----|
| NB | NB | NB | NM | NM | NS | ZO | ZO |
| NM | NB | NB | NM | NS | NS | ZO | PS |
| NS | NM | NM | NM | NS | ZO | PS | PS |
| ZO | NM | NM | NS | ZO | PS | PM | PM |
| PS | NS | NS | ZO | PS | PS | PM | PM |
| PM | NS | ZO | PS | PM | PM | PM | PB |
| PB | ZO | ZO | PM | PM | PM | PB | PB |

表 1 中变量及其取值代表物理量的大小及方向,并不代表反馈的正、负,这主要是为了便于编程。

其中,计算 e 时采用公式 $e = T_0 - T$, 式中 T_0 为工件的设定温度; T 为工件的测定温度。因此,从此表来看, e 为 NB 并不代表温度远低于设定值,而是正好相反的,因此 u 应取 NB。因此模糊规则表在字面上虽然与通常文献中所给出的模糊控制规则表不同,而实质上是一致的,并不违反负反馈规律,主要是为了编程的方便。

4 试验结果

电子束钎焊控制系统将电子束焊接的过程控制(包括抽真空过程、施加栅偏电压、加速电压、灯丝电压及启动束流)、电子束扫描轨迹控制、温度信号的采集与处理(得到偏差值及偏差的变化率)、工件温度模糊控制集成在一起,在自主研发的控制软件控制下形成一个高效、高精度的控制系统。该系统不仅能实现以上所述的各项控制功能,而且还可在控制过程中应用高速磁盘流技术实现数据的高速存储,将所需数据进行在线实时记录,以做分析之用。

试验条件,试件材料为 1Cr18Ni9Ti, 尺寸 $\phi 40\text{ mm} \times 3\text{ mm}$; 扫描轨迹为三叶形,如图 1 左侧第一列所示;扫描频率为 20 Hz;电子束加速电压为 60 kV。

图 4、5、6 为试验结果示例。

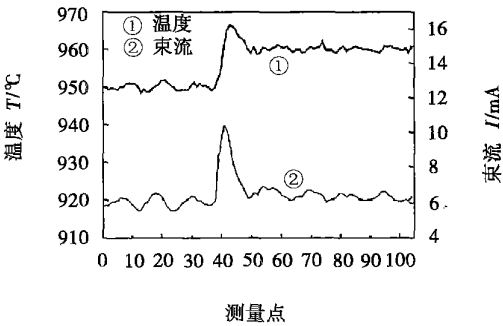


图 4 工件温度设定值 $950\text{ }^{\circ}\text{C} \rightarrow 960\text{ }^{\circ}\text{C}$

Fig. 4 Workpiece temperature set value $950\text{ }^{\circ}\text{C} \rightarrow 960\text{ }^{\circ}\text{C}$

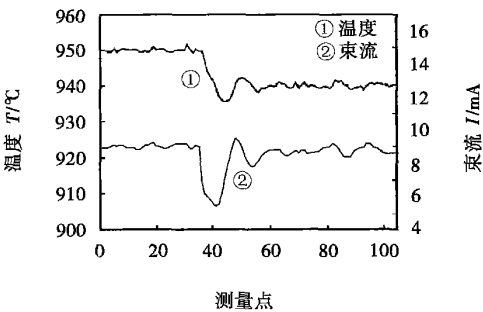


图 5 工件温度设定值 $950\text{ }^{\circ}\text{C} \rightarrow 940\text{ }^{\circ}\text{C}$

Fig. 5 Workpiece temperature set value $950\text{ }^{\circ}\text{C} \rightarrow 940\text{ }^{\circ}\text{C}$

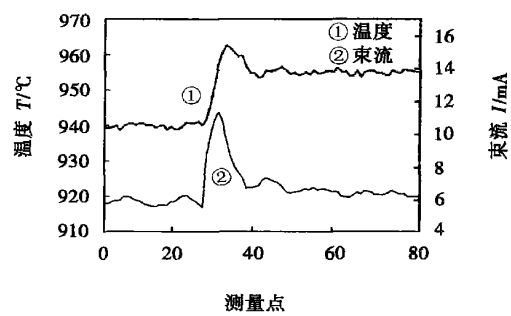


图 6 工件温度设定值 940 °C→955 °C
Fig. 6 Workpiece temperature set value 940 °C→955 °C

在图 4 中, 工件温度设定值初始为 950 °C, 经过升温过程后, 在模糊控制器的控制下在 950 °C 稳定下来, 然后给温度设定值一个 10 °C 的增量, 经过短暂的过渡过程后, 工件温度即在新的设定值 960 °C 附近稳定下来。图 4 中上一曲线为实时采集的工件温度变化过程, 下一曲线为实时记录的束流值, 上下两条曲线是相互对应的。

图 5 中, 初始温度设定值仍为 950 °C, 当工件温度达到稳定状态后, 给温度设定值一个 -10 °C 的增量, 从而检测温度设定值降低后系统的响应过程。

图 6 中, 温度设定值的变化量为 15 °C, 与图 4 相对比可以发现, 响应过程的超调量不但相当小, 而且对温度设定值的变化不敏感。

由图 4~图 6 中可以发现, 系统响应速度快, 稳定时间短, 超调量小, 稳态偏差小, 在过渡过程中都没有振荡, 系统的动、静态特性都是相当令人满意的。

由此可见, 以高能束流电子束为热源的电子束钎焊过程中, 虽然电子束流能量密度极高, 工件温度对束流值非常敏感, 而且系统本身十分复杂, 影响因

素众多, 但采用模糊控制器对其进行控制, 对于系统参数经常发生变化的电子束钎焊过程, 一方面是具有广泛的适应性, 另一方面, 所得到的控制特性非常理想。

5 结 论

全新地设计了电子束钎焊温度模糊控制系统, 系统集成电子束焊接过程控制、电子束扫描轨迹控制、工件温度模糊控制、过程数据高速采集与存储等多项功能, 控制系统具有响应速度快、稳定时间短、稳态误差小、超调量小等特点, 表明在以高能量密度的电子束为热源的电子束钎焊过程中采用模糊控制技术对被焊工件温度进行控制, 可以得到理想的控制效果。

参考文献:

[1] Jan Dupák, Ivan Věek, Martin Zobač. Electron gun for computercontrolled welding of small components[J]. Vacuum, 2001, 62(2-3): 159-164.
[2] Keitel Steffen, Sobisch Gotz, Hantke Andreas, et al. Shaping of deflection figures of electron beam equipment [J]. Schweissen und Schneiden/Welding &Cutting, 1998, 50(8): E150-E154
[3] Arata Y. Plasma, electron and laser beam technology[M]. Metals Park, Ohio: American Society for Metals, 1986.
[4] 王学东, 姚舜. 扫描轨迹可控的电子束钎焊[J]. 焊接学报, 2004, 25(6): 31-34.

作者简介: 王学东, 男 1969 年出生, 副教授, 博士研究生。研究方向为焊接过程自动控制, 发表论文 11 篇。

Email: wxue 2004@ yeah. net

The highest temperature appears near the lower surface. Comparison between the simulated results of the residual stress fields with measured ones shows that there is a good agreement with each other, which proves this model is effective. According to this model, the stresses at different time during cooling after hardfacing was simulated too by using the temperature field mentioned above. The results show that the tensile stress at the dangerous location appears at the interface, change of stress between the mutation is great.

Key words: hardfacing; temperature/stress field; residual stress; finite element method

Nitrogen and its second phase particles in low carbon Ti-Nb microalloyed weldable steels

YIN Gui-quan, WANG Shi-jun, HUANG Zhen-yi (School of Material Science and Engineering, Anhui Polytechnic University, Maanshan 243002, Anhui, China). p57—60, 64

Abstract: The effects of nitrogen content on austenite grain size at high temperature and impact toughness of simulated welding HAZ and actions of second phase particles (Ti, Nb)N in series low carbon Ti-Nb microalloyed weldable steels were studied. The simulated weld with great heat input had been carried out. The austenite grain size at high temperature was measured and impact toughness after welding was tested. Morphology and distribution characteristics of second phase particles (Ti, Nb)N in typical specimens had been observed by using transmission electron microscope by means of carbon extraction replicase technique. The results showed that there is good correspondence among Ti and N content, size of particles (Ti, Nb)N, austenite grain size and impact toughness. Toughness after welding is improved because of formation of fine and dispersive second phase particles (Ti, Nb)N which refines austenite grain size at high temperature. There is a scope of rational N content in low carbon Ti-Nb microalloyed weldable steels.

Key words: low carbon Ti-Nb microalloyed weldable steels; nitrogen content; second phase particles (Ti, Nb)N; austenite grain size; impact toughness

A novel instrument of silicon chip thermocompression outer wire bonding and jointing process research

WANG Quan¹, DING Jian-ning¹, XUE Wei², LING Zhi-yong¹ (1. School of Mechanical Engineering, Jiangsu University, Zhenjiang 212013, Jiangsu, China; 2. Industrial Engineering School, Wenzhou University, Wenzhou 325035, Zhejiang, China). p61—64

Abstract: In the process of piezoresistive pressure sensor packaging, the thermocompression wire bonding was studied to meet the outer interconnection of silicon gauge. A novel instrument of thermocompression wire bonding was developed. Microstructures of the joint interface were analyzed by SEM. The thermocompression wire bonding strength was tested with bonding tester. The strength was over 0.17 N. Through the investigation of the metallic compound in the interface of Au-Al and increasing of its diffusion depth

with temperature, the temperature of substrate was kept between 150 °C and 200 °C and the temperature of the solder chisel was kept at about 150 °C in operation. The interface of thermocompression point was tested with good reliability. The instrument was easy to be operated and fitted for batch fabrication of piezoresistive pressure sensor.

Key words: piezoresistive pressure sensor; wire bonding; thermocompression bonding; gold wire

Structure investigation of friction stir welding of 7A52 aluminum alloy

FU Zhi-hong^{1,2}, HE Di-qiu², ZHOU Peng-zhan², HU Ai-wu¹ (1. Hunan Polytechnic University, Zhuzhou 412008, Hunan, China; 2. College of Mechanical and Electric Engineering, Center South University, Changsha 410083, China). p65—68

Abstract: The macro- and micro-structures and micro-hardness of friction stir welding of 7A52 aluminum alloy were investigated. The welded joint of aluminum alloy 7A52 can be divided into three regions as follows: heat affected zone (HAZ), thermo-mechanically affected zone (TMAZ) and weld nugget. The weld nugget had a dynamic recrystallized fine isometric crystal structure. The TMAZ had a highly deformed structure, and the grains were curved strip and larger than that in the weld nugget. The HAZ had similar structure to the base metal, but the size of grains was larger than that in the base metal. Distribution of microhardness in the cross section presented a trend of high-low-high-low-high. The base metal outside the weld show the maximal hardness, and the top of the weld nugget has the same hardness as the base metal, the lowest hardness was in the advancing side in the HAZ.

Key words: friction stir welding; weld; structure; hardness

Effects of parameters of U-I mode pulsed MAG on droplet transfer

LU Zhen-yang, HUANG Peng-fei, LIAO Ping, YIN Shu-yan (School of Mechanics and Electricity, Beijing University of Technology, Beijing 100022, China). p69—72

Abstract: The U-I mode inverter P-MAG welding machine controlled by 80C196KC 16-bit single chip computer was designed. By sampling the voltage and current of arc in the welding process, the arc voltage is kept constant in the peak period and welding current is kept constant in the base period. Arc length self-adjustment was realized by changing of the peak current, and the pulse parameter was optimized to make sure the one pulse one droplet transfer mode. The experimental result indicated that the welding machine has perfect welding performance.

Key words: voltage-current mode; single chip computer; pulse metal active-gas welding

Electron beam brazing temperature fuzzy control system

WANG Xue-dong, YAO Shun (School of Materials Science and Engineering, Shanghai Jiaotong University, Shanghai 200030, China). p73—76

Abstract: The workpiece temperature fuzzy control technology was used in the electron beam brazing process. The system integrated EBW process control, electron beam scanning track control, workpiece temperature fuzzy control, welding data high-speed acquisition and storage. Through the programming and control of the electron beam scanning tracks, the energy input requirements of curve brazing joints with various shapes could be satisfied. During the scanning and heating process with the electron beam, the temperature signals of the workpiece were obtained on-line and compared with the set value, so as to get the error and the error change rate of the joint temperature, which acted as the two inputs of the fuzzy controller. The fuzzy controller gave appropriate control amounts according to its inputs to adjust the electron current, and the closed-loop control of brazing temperature was realized. The experiment results showed that ideal control characters could be obtained if fuzzy control technology was used in the electron beam brazing process. The control system had fast response speed, short settle time, small steady-state error and small overshoot.

Key words: electron beam brazing; scanning track; temperature field closed-loop control; fuzzy control

Properties of maraging steel hardfacing metal deposited by metal powder-cored wire

FANG Jian-jun, LI Zhuo-xin, WEI Qi, HU Qiang (School of Mechanics and Electrical Engineering, Beijing University of Technology, Beijing 100022, China). p77—80

Abstract: Hardfacing material of maraging steel metal powder-cored wire was deposited by pulse TIG on aluminum die cast dies to improve the dies' properties and extend its service life. Microstructure and phase characteristics were analyzed by using SEM, TEM and XRD. After aging, the metal got super-high strength, hardness and thermal fatigue resistance by intermetallic compound $[\text{Ni}_3\text{Ti}, \text{Ni}_3(\text{Al}, \text{Ti})]$ precipitating in Fe matrix. Metastable phases such as $(\text{Ni}_{2.9}\text{Fe}_{0.1})/\text{Ti}$ and $(\text{Ni}_{0.7}\text{Fe}_{0.3})$ were found. Thermal fatigue experimental results showed that maraging steel deposited by metal-cored wire has higher thermal fatigue resistance properties than that of H13 solid wire and 18Ni maraging steel.

Key words: pulse tungsten inert-gas welding; maraging steel; metal powder-cored wire; intermetallic compound; thermal fatigue resistance

Computer aided programming in offline programming systems of welding robots

HE Guang-zhong, GAO Hong-ming, ZHANG Guang-jun, WU Lin (State Key Laboratory of Advanced Welding Production Technology, Harbin Institute of Technology, Harbin 150001, China). p81—84

Abstract: An approach by interfacing a feature modeler of welded structure and an arc welding expert system to provide the automatic generation of welding paths and the corresponding technology data was proposed. The prototype system was developed in Solid-Works. An arc welding expert system can automatically generate

welding process parameters. Its input data came from the feature modeler of welding part. It combined case-based reasoning with artificial neural networks methods to deal with the welding process design. Several network modules were developed to learn from welding process database based on back-propagation neural networks.

Key words: offline programming; auto planning; feature modeling; welding parameter planning

Brazing between high purity alumina ceramics and titanium

ZHAO Wen-qing, WU Ai-ping, ZOU Gui-sheng, LIU Gen-mao (Department of Mechanical Engineering, Tsinghua University, Beijing 100084, China). p85—88

Abstract: The joints of high purity alumina ceramics and Ti metal with high strength and tightness are needed in electron tube. The joints with shear strength higher than 100 MPa could be achieved by brazing with Ag-Cu-Ti at the temperature of 825—875 °C and the holding time of 15—20 min. Lower or higher temperature and shorter or longer holding time are detrimental to joint strength, and the joint strength decreased when the ceramic surface was abraded. The joint consisted of Al_2O_3 /reaction layer/Cu-Ti compounds+Ag/ α -Ti (Cu)/Ti. The main products in the reaction layer were $\text{Cu}_3\text{Ti}_3\text{O}$ and Cu_4Ti .

Key words: high purity alumina ceramics; titanium; brazing; joint microstructures; joint shear strength

Analysis of microstructure and mechanical properties of Be/Al weld

HAO Guo-jian, LIN Zhijun, LIN Jun-pin, WANG Yan-li, CHEN Guo-liang (State Key Laboratory for Metals and Materials, Beijing University of Science and Technology, Beijing 100083, China). p89—92

Abstract: Microstructure and mechanical properties of Be/Al weld were analyzed with nano indenter. The results showed that there are beryllium phases embedded in the aluminum matrix in the fusion zone. The microstructure of the fusion zone is low melting point phase that enlarged the region of weld solidification temperature and brought great thermal stress, especially at the side of beryllium. There are the certain gradients of microhardness and elastic modules at the interface of Be/Al welded joint. The microhardness and elastic modules are not stable at beryllium side of joint zones, which indicates that there exist brittle phase at heat affected zone. So the welding cracks nucleated easily at beryllium side of welding zone.

Key words: nano indenter; eutectic structure; Be/Al; mechanical property; laser welding

Temperature field of arc gouging and its influence on microstructures

HU Jun-feng¹, YANG Jian-guo¹, FANG Hong-yuan¹, LI Guang-min², CHEN Wei¹ (1. State Key Laboratory of Advanced Welding Production Technology, Harbin Institute of Technology, Harbin 150001, China; 2. Bohai Shipbuilding Heavy Industry Co Ltd, Huludao 125004, Liaoning, China). p93—96